

1 Exploring an approximation for the homogeneous freezing temperature of water
2 droplets

3

4

5 K. -T. O¹, R. WOOD¹

6 [1] University of Washington, Department of Atmospheric Sciences, Seattle, WA,
7 USA

8

9

10

11

12

13

14

15

16

17

18

19

20

21

22

23

24

25

26

27 Corresponding author:

28 Kuan-Ting O

29 408 Atmospheric Sciences–Geophysics (ATG) Building

30 Box 351640, Seattle, Washington 98195-1640

31 Phone (206) 543-4250 | Fax (206) 543-0308

32 ktoandy@u.washington.edu

33 **Abstract**

34 In this work, based on the well-known formulae of classical nucleation theory
35 (CNT), the temperature $T_{N_c=1}$ at which the mean number of critical embryos inside a
36 droplet is unity is derived from the Boltzmann distribution function and explored as
37 an approximation for homogeneous freezing temperature of water droplets. Without
38 including the information of the applied cooling rate $\gamma_{cooling}$ and the number of
39 observed droplets $N_{total_droplets}$ in the calculation, the approximation $T_{N_c=1}$ is able to
40 reproduce the dependence of homogeneous freezing temperature on drop size V and
41 water activity a_w of aqueous drops observed in a wide range of experimental studies
42 for droplet diameter $> 10 \mu\text{m}$ and $a_w > 0.85$, suggesting the effect of $\gamma_{cooling}$ and
43 $N_{total_droplets}$ may be secondary compared to the effect of V and a_w on
44 homogeneous freezing temperatures in these size and water activity ranges under
45 realistic atmospheric conditions. We use the $T_{N_c=1}$ approximation to argue that the
46 distribution of homogeneous freezing temperatures observed in the experiments may
47 be partly explained by the spread in the size distribution of droplets used in the
48 particular experiment. It thus appears that the simplicity of this approximation makes
49 it potentially useful for predicting homogeneous freezing temperatures of water
50 droplets in the atmosphere.

51

52

53

54

55

56 Keywords: classical nucleation theory, homogeneous ice nucleation, freezing
57 temperature

58 1. Introduction

59 Since the summary article of McDonald (1953), it has been widely observed that
60 ice nucleation of water droplets does not occur at the ice melting temperature (e.g.
61 273.15 K at 1atm), and liquid water is frequently observed in clouds as cold as to 238
62 K (Rosenfeld and Woodley, 2000; Hu et al., 2010). Laboratory observations of
63 homogeneous ice nucleation in pure water generally show that all droplets do not
64 freeze at exactly the same temperature, and that the fraction of droplets that freeze in
65 a given time is a function of temperature and time (hereafter we refer to this type of
66 experiment as a *fraction experiment*) (e.g. Bigg 1953; Carte 1956; Broto and Clause,
67 1976; Earle et al., 2010; Riechers et al., 2013). Here, experimental data of the freezing
68 temperatures of pure water droplets from 15 independent studies over the past 60
69 years are collected (Fig. 1 and Table 1), showing a clear dependence of freezing
70 temperature upon drop volume across different experiments. Over the investigated
71 size interval (1-1000 μm diameter), observed freezing temperatures range from 232 K
72 to 240 K. The range of freezing temperatures and the volume dependence in Fig. 1 are
73 consistent with the experimental data reviewed in Pruppacher (1995).

74 On the other hand, solutes, at sufficiently high concentrations, can suppress the
75 homogeneous freezing temperature of water droplets. Koop et al. (2000) showed that
76 the depression of freezing temperature strongly depends on the water activity a_w of
77 the solution droplet, which has been confirmed in several independent experimental
78 studies (e.g. Knopf and Lopez, 2009; Knopf and Rigg, 2011). In this paper, two
79 aforementioned features of homogeneous ice nucleation observed in the experimental
80 data are examined – (1) the volume and water activity dependence of homogeneous

81 freezing temperatures of water droplets $T_f(V, a_w)$; (2) the distribution of
82 homogeneous freezing temperatures observed in fraction experiments $f(T_f)$. In this
83 paper, we describe only volume-based nucleation and do not include the droplet
84 surface effects on homogeneous ice nucleation as there remains considerable
85 uncertainty about the importance of surface nucleation (Kay et al., 2003; Duft and
86 Leisner, 2004). The unified explanations of the observed dependencies of the
87 homogeneous freezing temperature on droplet size and water activity have been
88 proposed by several studies based on different theoretical frameworks such as ice
89 nucleation rate J and density fluctuation (e.g. Pruppacher 1995; Baker and Baker
90 2004; Khvorostyanov and Curry 2009; Barahona 2014). In our study, based on a
91 cornerstone of classical nucleation theory (CNT), namely that a critical embryo
92 existing in a droplet triggers ice crystal formation, we explore a simple approximation
93 for the homogeneous freezing temperature, and seek a simpler parameterization to
94 describe homogeneous ice nucleation process in the atmosphere. Section 2 describes
95 the approximation; Section 3 gives the comparisons between the theoretical estimates
96 and the experimental data; Section 4 is the discussion; Section 5 is the summary.

97

98

99

100

101

102

103

104 **2. Background**

105 **2.1 The approximation** $T_{N_c=1}(V, a_w)$

106 According to CNT, the formation of a critical embryo inside a droplet can trigger
107 the freezing process in the droplet. The critical embryo defined as the i -mers having
108 the highest formation energy is formed by the critical fluctuation in orientation of
109 hydrogen bonds (e.g. density fluctuation) (Baker and Baker 2004), which is large
110 enough to provide the formation energy of the critical embryo $\Delta F_c(T, a_w)$ and
111 remove metastability of supercooled water. The probability of occurrence of the
112 critical fluctuation is $\exp(\frac{-\Delta F_c(T, a_w)}{k_B T})$ (Landau and Lifshitz, 1980, P.472-473;
113 Pruppacher and Klett, 1997), and thus the *mean number* of the critical embryos inside
114 a water droplet in thermal equilibrium can be predicted by a Boltzmann distribution
115 (Landau and Lifshitz, 1958, P.107; Vali, 1999),

116
$$N_{c_mean}(V, a_w, T) = V\rho \exp(\frac{-\Delta F_c(T, a_w)}{k_B T}) \quad (1)$$

117 where V is the volume of the droplet, ρ is the number density of water molecules,
118 k_B is Boltzmann's constant, T is the temperature of the droplet, and $\Delta F_c(T, a_w)$ is
119 the formation energy of the critical embryo in the droplet with water activity a_w at
120 T , which will be discussed in detail in Sect. 2.2. The Boltzmann distribution form of
121 the critical embryo is derived from the partitioning function of the grand canonical
122 ensemble, and it should be noted that the derived particle number of the Boltzmann
123 distribution function is not a "constant" but is a "mean" number (detailed derivation
124 and explanations can be found in Landau and Lifshitz, 1958, P.107 and Sadvskii,
125 2012, Chapter 3.1).

126 The total freezing time $\tau_{freezing}$ of a water droplet can be split conceptually into
 127 three stages – (1) $\tau_{meta_remove} (\sim \frac{1}{J})$ the time needed for the occurrence of the critical
 128 fluctuation (2) $\tau_{formation}$ the time needed to form a critical embryo and (3) $\tau_{growing}$
 129 the growing time for the critical embryo expanding to the whole droplet body. These
 130 depend on V , a_w and T of the droplet (Pruppacher and Klett 1997; Bauerecker et
 131 al., 2008). To observe freezing of droplets with volume V and water activity a_w
 132 occurring at temperature T , the residence time of freezing experiments $\tau_{residence}$ at
 133 T has to be longer than $\tau_{freezing}(V, a_w, T)$, resulting in a dependence of the
 134 homogeneous freezing temperature on the cooling rate $\gamma_{cooling}$ of droplets in principle.
 135 According to the theoretical estimates (see Pruppacher and Klett 1997, P.678), the
 136 time scale of $\tau_{formation} + \tau_{growing}$ for the size of the droplets investigated here is short
 137 compared with the typical residence times in the laboratory studies. Thus, the
 138 dominant factor determining the homogeneous freezing temperatures is τ_{meta_remove} .
 139 Because τ_{meta_remove} is the time needed for the occurrence of the critical fluctuation
 140 among water molecules, τ_{meta_remove} is shorter in a larger droplet with more
 141 molecules $V\rho$ or at lower temperature when the fluctuation probability
 142 $\exp(\frac{-\Delta F_c(T, a_w)}{k_B T})$ is higher; $\tau_{meta_remove}^{-1} \propto N_{c_mean}(V, a_w, T)$. Embryo interaction is a
 143 stochastic process and $N_{c_mean}(V, a_w, T)$ simply expresses the mean state, so there is
 144 always a spread of τ_{meta_remove} among droplets even in a idealized case that all the
 145 droplets used in the experiment have exactly the same V and a_w and are at exactly
 146 the same temperature T . The spread of τ_{meta_remove} can be wider when there are
 147 more observed droplets $N_{total_droplets}$, which in principle can explain the fraction

148 experiments that some droplets with shorter τ_{meta_remove} can always be frozen at
 149 higher temperature, or in shorter time for droplets at the same temperature even when
 150 the droplets have a monodisperse size distribution and exactly same a_w . Hereafter we
 151 refer the distribution of homogeneous freezing temperatures owing to $N_{total_droplets}$
 152 when all the droplets have exactly same V and a_w as a *stochastic feature*. Based
 153 on above-mentioned principles, the homogenous freezing temperature of water
 154 droplets and τ_{meta_remove} can each be written as a function of V , a_w , $\gamma_{cooling}$ and
 155 $N_{total_droplets}$, namely $T_f(V, a_w, \gamma_{cooling}, N_{total_droplets})$ and
 156 $\tau_{meta_remove}(V, a_w, \gamma_{cooling}, N_{total_droplets})$.

157 Koop et al. (1998) reported that observed homogeneous freezing temperatures do
 158 not significantly depend on $\gamma_{cooling}$ of the droplets for $\gamma_{cooling}$ smaller than 20 K min^{-1}
 159 (corresponding to vertical velocities 33.3 m s^{-1} in clear air). The results of Koop et al.
 160 (1998) actually indicate that the slope of $\frac{\partial \tau_{meta_remove}}{\partial T}$ is very steep at the temperature
 161 when the scale of τ_{meta_remove} is close to $\tau_{residence}$ in most practical experiments and
 162 realistic atmospheric conditions, resulting in the small dependence of T_f on $\gamma_{cooling}$
 163 as suggested by Brewer and Palmer (1951). Based on that, in most of the practical
 164 freezing experiments and realistic atmospheric conditions ($\gamma_{cooling} < 20 \text{ K min}^{-1}$), the
 165 observed homogeneous freezing temperatures can be considered as a threshold
 166 temperature when $\frac{\partial \tau_{meta_remove}}{\partial T} \rightarrow \infty$. In this study, we intend to find this threshold
 167 temperature directly from the information given by $N_{c_mean}(V, a_w, T)$. The number of
 168 critical embryos derived from the Boltzmann distribution is a mean value and does
 169 not provide any information regarding freezing time, so it can not be used to study the

170 dependence of the homogeneous freezing temperature on cooling rate (i.e. time
 171 dependence) and number of droplets used in the experiments (i.e. stochastic feature).
 172 Nevertheless, since the formation of one critical embryo is required to trigger the ice
 173 nucleation process in a droplet, $T_{N_c=1}$ may be a good approximation for the threshold
 174 temperature, the temperature at which the mean number of the critical embryos inside
 175 a droplet is unity, which can be given by

$$176 \quad N_{c_mean} = 1 = V \rho \exp\left(\frac{-\Delta F_c(T_{N_c=1}, a_w)}{k_B T_{N_c=1}}\right) \quad (2)$$

177 According to the formula of $\Delta F_c(T, a_w)$, $T_{N_c=1}$ is determined by V and a_w of
 178 the droplet, namely $T_{N_c=1}(V, a_w)$. Figure 2 shows the mean number of critical
 179 embryos inside a pure water droplet ($a_w = 1$) at different temperatures using Eq. (1)
 180 (see next section for details of $\Delta F_c(T, a_w)$ used in the calculation). It indicates that
 181 smaller droplets require lower temperatures to reach the state that $N_{c_mean} = 1$,
 182 showing the volume dependence of $T_{N_c=1}(V, a_w)$. Figure 3 shows the mean number of
 183 critical embryos inside a solution droplet with different values of water activity. The
 184 result indicates that more concentrated solution droplets (lower a_w) need lower
 185 temperature to reach the state that $N_{c_mean} = 1$. This represents the solution effect on
 186 $T_{N_c=1}(V, a_w)$. The sensitivity of $T_{N_c=1}(V, a_w)$ to the variation of diameter δd and
 187 water activity δa_w of droplets can be written as

$$188 \quad \delta T_{N_c=1} = \frac{\partial T_{N_c=1}}{\partial a_w} \delta a_w + \frac{\partial T_{N_c=1}}{\partial \log_{10} d} \delta \log_{10} d \quad (3)$$

189 where d is the diameter of droplet (μm). As shown in Fig. 1, the dependence of
 190 $T_{N_c=1}$ on $\log_{10} d$ is nearly linear, so the decadal log is used here to simply derive the

191 linear dependence. The values of $\frac{\partial T_{N_c=1}}{\partial a_w}$ and $\frac{\partial T_{N_c=1}}{\partial \log_{10} d}$ are about 216 K and 2.5 K
 192 respectively over the investigated interval of water activity and drop size, which are
 193 derived numerically from Eq. (2).

194 2.2 Formation energy of the critical embryo $\Delta F_c(T, a_w)$

195 The formation energy of the critical embryo $\Delta F_c(T, a_w)$ can be written as

$$196 \Delta F_c = \frac{1}{3} s \sigma_{i/w}(T, a_w) r_c^2 \quad (4)$$

$$197 r_c = \frac{2 \sigma_{i/w}(T, a_w) v_1^{water}}{k_B T \ln\left(\frac{e_{sw} a_w}{e_{si}}\right) + k_B T \ln(a_w)} \quad (5)$$

198 where $\sigma_{i/w}(T, a_w)$ is the interfacial energy between liquid water and solid ice, s is
 199 the shape factor of the embryo (~ 21 by assuming the shape is hexagonal prism), r_c
 200 is the radius of the critical embryo, v_1^{water} is the volume of single water molecule,
 201 e_{sw} and e_{si} are the saturation vapor pressures over water and ice respectively
 202 (Murphy and Koop, 2005), and a_w is the water activity of the solution droplet (see
 203 detailed derivations of Eq. (4) in Defour and Defay, 1963 and Pruppacher and Klett,
 204 1997). It should be noted that the term $k_B T \ln(a_w)$ in r_c (Eq. (5)) is the *entropy of*
 205 *unmixing* which originates from the change of the Gibbs free energy of the bulk
 206 solution during freezing, and is usually neglected in the previous theoretical studies
 207 (Bourne and Davey, 1976; Black 2007). Barahona (2014) pointed out that although
 208 this term is small for dilute solution, it should not be neglected when applying to high
 209 concentration solution droplets (see Eq. (8) in Barahona (2014)).

210 The value of interfacial energy between liquid water and solid ice $\sigma_{i/w}(T, a_w)$ is
 211 needed for our calculation of Eq. (4) and (5). As most studies suggest that the

212 temperature dependence of $\sigma_{i/w}(T, a_w)$ should be linear (Ickes et al., 2015), and that
 213 increasing the concentration of the solution droplet increases the value of $\sigma_{i/w}(T, a_w)$
 214 (Jones and Chadwick, 1971; Alpert et al. 2011), $\sigma_{i/w}(T, a_w)$ can be written as

$$215 \quad \sigma_{i/w}(T, a_w) = \sigma_{i/w,e} + \frac{\partial \sigma_{i/w}}{\partial T}(T - T_0) + \frac{\partial \sigma_{i/w}}{\partial a_w}(1 - a_w) \quad (6)$$

216 where $\sigma_{i/w,e}$ is the interfacial energy at the equilibrium temperature of pure ice-water,
 217 and T_0 is the equilibrium temperature. The direct measurement of $\sigma_{i/w}(T, a_w)$ is
 218 extremely difficult, so most of the estimations are based on combinations of CNT and
 219 laboratory measurements of T_f and observed freezing rate to retrieve the values of
 220 $\sigma_{i/w}(T, a_w)$ (e.g. Zobrist et al., 2007; Murray et al., 2010). These studies have shown
 221 considerable diversity in the reported estimations of $\sigma_{i/w}(T, a_w)$ (Ickes et al., 2015).

222 Instead, we use values of $\sigma_{i/w,e}$ and $\frac{\partial \sigma_{i/w}}{\partial T}$ derived from a state-of-the-art molecular
 223 dynamics model that explicitly simulates the molecular configurations under
 224 supercooling conditions. Benet et al. (2014) gives values of $\sigma_{i/w,e}$ from the TIP4P
 225 water model ($\sigma_{i/w,e} = 26.5 \times 10^{-3} \text{ J m}^{-2}$), TIP4P/2005 water model ($\sigma_{i/w,e} = 27 \times 10^{-3} \text{ J m}^{-2}$),
 226 and TIP4P-Ew water model ($\sigma_{i/w,e} = 27.5 \times 10^{-3} \text{ J m}^{-2}$), and these three values will all be
 227 used in our calculations. According to Ickes et al. (2015), the values of the interfacial
 228 energy used here are about the median of all the values derived from the previous
 229 studies. Regarding $\frac{\partial \sigma_{i/w}}{\partial T}$, Espinosa et al. (2014) provided an average value of $0.25 \times$
 230 $10^{-3} \text{ (J m}^{-2} \text{ K}^{-1})$ from three different water molecular models (TIP4P/ICE, TIP4P and
 231 TIP4P/2005) down to a supercooling of about 30K. Regarding $\frac{\partial \sigma_{i/w}}{\partial a_w}$, Barahona
 232 (2014) proposed a new thermodynamic framework approximating the interfacial
 233 energy of ice-solution by assuming the interface between solid ice and liquid water is

234 made of liquid molecules trapped by the solid matrix, which gives the relationship
 235 between $\sigma_{i/w}$ and a_w . Based on this approximation, the solution effect on the
 236 interfacial energy can be written as

$$237 \quad \frac{\partial \sigma_{i/w}}{\partial a_w} = - \frac{\Gamma_w^2 s_{area} k_B T \frac{1}{a_w}}{(36\pi(v_1^{water})^2)^{1/3}} \quad (7)$$

238 where Γ_w is the surface excess of water (~ 1.46) (Spaepen 1975) and s_{area} is the
 239 surface area parameter ($\sim 1.105 \text{ mol}^{2/3}$) (see Barahona 2014 for details). The values of
 240 $\sigma_{i/w}(T, a_w)$ estimated from above studies are used to derive the numerical result
 241 $T_{N_c=1}(V, a_w)$ presented here.

242 **3. Results – Comparison between the approximation and the experimental data**

243 **3.1 Volume and water activity dependence of $T_f(V, a_w)$**

244 To test our approximation, we aim to compare the observed $T_f(V, a_w)$ and
 245 $f(T_f)$ with $T_{N_c=1}(V, a_w)$ derived using the constraint in Eq. (2). First,
 246 $T_{N_c=1}(V, a_w = 1)$ of pure water droplet is derived. Figure 1 shows the comparison
 247 between the experimentally determined homogeneous freezing temperatures
 248 $T_f(V, a_w = 1)$ (details of the experiments are provided in Table 1) and the
 249 approximations $T_{N_c=1}(V, a_w = 1)$. For droplet diameters $> 10\mu\text{m}$, the theoretical values
 250 of $T_{N_c=1}(V, a_w = 1)$ derived by the value of $\sigma_{i/w,e}$ from TIP4P water model agree very
 251 well with most of the experimental data $T_f(V, a_w = 1)$. Using the values of $\sigma_{i/w,e}$
 252 from TIP4P/2005 and TIP4P-Ew leads to a shift downward of about 1~2 K of
 253 $T_{N_c=1}(V, a_w = 1)$. There is one study regarding the time dependence should be
 254 mentioned. The laboratory observation of Murray et al. (2010) (black triangle in Fig.
 255 1) showed that varying of cooling rate from 2.5 K min^{-1} to 10 K min^{-1} corresponds to a

256 shift of 0.5 K to 1 K in observed freezing temperatures of pure water droplets, and our
 257 best agreement estimates $T_{N_c=1}(V, a_w = 1)$ can only explain the experimental data with
 258 slowest cooling rate (2.5 K min⁻¹). The finding of Murray et al. (2010) will be
 259 discussed in Sect. 4. For droplets smaller than 10 μm (diameter), there are obvious
 260 deviations of observed freezing temperatures among the experimental studies. These
 261 studies do not provide enough information regarding $\gamma_{cooling}$, $N_{total_droplets}$ and the
 262 spread in drop size, so we cannot evaluate what causes the disparity. We suggest that
 263 freezing experiments of pure droplets smaller than 10 μm (diameter) need more
 264 refinement and should report the potentially important dependencies such as applied
 265 cooling rate, size distribution of droplets and number of observed droplets used in
 266 experiments.

267 Second, the solution effect on homogeneous freezing temperature $T_f(V, a_w)$ is
 268 explored by changing the water activity in Eq. (5) and (6) to derive the approximation
 269 $T_{N_c=1}(V, a_w)$, which will be compared with the experimental data collected in Koop et
 270 al. (2000), Knopf and Lopez (2009) and Knopf and Rigg (2011). Size of the droplets
 271 used in the collected experimental data ranges from 1 μm to 10 μm in Koop et al.
 272 (2000), from 10 μm to 80 μm in Knopf and Lopez (2009) and from 20 μm to 80 μm in
 273 Knopf and Rigg (2011), and these sizes are included to calculate the approximation
 274 $T_{N_c=1}(V, a_w)$. Figure 4 shows the comparison between the experimental data and the
 275 approximation $T_{N_c=1}(V, a_w)$. Without considering the time dependence ($\gamma_{cooling}$
 276 varying from 1 K min⁻¹ to 10 K min⁻¹ among all the experiments) and the stochastic
 277 feature (i.e. $N_{total_droplets}$), the result shows that the approximation $T_{N_c=1}(V, a_w)$ is in
 278 good agreement with the experimental data for $a_w > 0.85$. The scattering of the

279 experimental data between the theoretical estimates for $a_w > 0.85$ (i.e. $T_{N_c=1}$ for
280 $d=1$ to $80 \mu\text{m}$) suggests that the spread of droplet size applied in the experiments
281 may play an important role in the spread of homogeneous freezing temperatures. For
282 the solution droplets with high concentration ($a_w < 0.85$), the observed freezing
283 temperatures show considerable spread. Abbatt et al. (2006) suggests that the disparity
284 of the experimental data for low a_w can be partly attributed to a variety of
285 heterogeneous process, which can result in the higher observed freezing temperatures.
286 In addition, as suggested by Knopf and Lopez (2009), the deviations at low water
287 activity may be most likely due to our incomplete understanding of a_w for certain
288 aqueous solutions and the corresponding uncertainties. Future experimental study is
289 suggested to focus on the freezing process of solution droplets with high solute
290 concentration ($a_w < 0.85$) to clarify the causes of the disparity.

291 Regarding the experimental uncertainty, Knopf and Lopez (2009) reported that
292 the value of a_w for supercooled aqueous solutions has the experimental uncertainty
293 δa_w of about ± 0.01 , which can result in the variation in $T_{N_c=1}$ of about ± 2 K based
294 on Eq. (3). Riechers et al. (2013) reported that the size of droplets produced by the
295 microfluidic device used in their experiment has three standard deviations (99.7%) of
296 about $18 \mu\text{m}$ to $33 \mu\text{m}$ in diameter, which can cause the variation in $T_{N_c=1}$ of about \pm
297 0.2 K to ± 0.5 K based on Eq. (3). Therefore, the variation in $T_{N_c=1}$ caused by the
298 experimental uncertainties δa_w and δd can be both substantial and should not be
299 neglected. We suggest future experimental studies should provide detailed
300 information regarding experimental uncertainties δa_w and δd for the purpose of
301 better constraining the observed freezing temperatures.

302 **3.2 Fraction of frozen pure water droplets as a function of temperature** $f(T_f)$

303 To further examine the application of $T_{N_c=1}(V, a_w)$ in homogeneous ice
304 nucleation, $T_{N_c=1}(V, a_w)$ is compared to the experimental data of the fraction
305 experiment of Riechers et al. (2013). According to CNT, the stochastic feature of the
306 ice nucleation process can basically explain the distribution of freezing temperatures
307 observed in the fraction experiment (Pruppacher and Klett, 1997, Eq. (7-71); Koop et
308 al., 1998; Niedermeier et al., 2011). However, current technology to produce water
309 droplets for such experiments introduces a spread of sizes, and the freezing
310 temperatures show a clear dependence on droplet volume (Fig. 1), so the spread in
311 sizes of water droplets used in the experiments may be important for explaining the
312 distribution $f(T_f)$. In other words, the size distribution of droplets used in a given
313 experiment may be an important factor governing the observed spread of freezing
314 temperatures (i.e. dotted line shown in Fig. 1). To test this, we incorporate the
315 reported droplet size distribution width into the numerical calculation. Unique among
316 such studies, Riechers et al. (2013) report both the spread of homogeneous freezing
317 temperatures and the mean μ and standard deviation σ of droplet size. According to
318 Eq. (3), the spread in the size distribution of water droplets will result in a spread in
319 the fraction of frozen droplets because larger droplets have higher $T_{N_c=1}(V, a_w)$ (i.e.
320 require less supercooling to freeze). Given the droplet size width, the distribution of
321 the approximations $T_{N_c=1}(V, a_w)$ of droplets can be derived from Eq. (2). Given a
322 Gaussian distribution of drop sizes, we estimate the fraction of drops that will freeze
323 at a given temperature *solely by assuming that the spread in freezing temperatures*
324 *arises from the spread in droplet sizes* based on Eq. (3). For example, we estimate

325 $T_{N_c=1}(V, a_w)$ of the droplets with size of $\mu+3\sigma$ (\sim the largest 0.15% of the drops) as
 326 the theoretical onset freezing temperature T_f^{onset} , $T_{N_c=1}(V, a_w)$ of the droplets with
 327 size of $\mu+1.64\sigma$ (\approx the largest 10% of the drops) as the theoretical estimates $T_f^{10\%}$,
 328 $T_{N_c=1}(V, a_w)$ of the droplets with mean size as the theoretical estimates $T_f^{50\%}$, and
 329 $T_{N_c=1}(V, a_w)$ of the droplets with size of $\mu-1.64\sigma$ (\approx the smallest 10% of the drops) as
 330 the theoretical estimates $T_f^{90\%}$, and $T_{N_c=1}(V, a_w)$ of the droplets with size of $\mu-3\sigma$ (\approx
 331 the smallest 0.15% of the drops) as the theoretical estimates T_f^{end} . The results
 332 presented in this section only use the value of $\sigma_{i/w,e}$ from the TIP4P water model,
 333 which has the best agreement with the experimental data shown in Sect. 3.1 (Fig. 1).

334 There are five experimental results from Riechers et al. (2013), each with
 335 different μ and σ . The comparisons (Fig. 5 and Table 2) show that our estimates
 336 match the experimental data fairly well. The slope of the freezing fraction versus
 337 temperature in the theoretical results is driven entirely by the reported spread in the
 338 size distribution of drops and matches fairly well with the observed slope, although
 339 across the experiments the theoretical slope is somewhat greater (observed values are
 340 shifted to the right of the blue curve at the higher temperatures but mostly to the left at
 341 the lower temperature), which might be attributable to the stochastic feature of the ice
 342 nucleation process. That said, the observational uncertainties in the experimental
 343 values of T_{on-set} , $T_{10\%}$, $T_{50\%}$ and $T_{90\%}$ more or less span the theoretical values
 344 derived from Eq. (2). Riechers et al. (2013) also reported that during cooling, the
 345 majority of the droplets are frozen over a temperature interval of 0.84-0.98 K, which
 346 is consistent with the range between the theoretical estimates T_f^{onset} and T_f^{end} derived
 347 here, namely 0.42-1.06 K from five different droplet size distributions, suggesting the

348 spread in droplet size (i.e. a disperse distribution) may be an important factor
349 governing the spread of the homogeneous freezing temperatures observed in a given
350 fraction experiment.

351 The comparison made in Sect. 3.1 to 3.2 shows that the distribution of the
352 freezing temperatures among the data can mostly be explained by the dependence of
353 $T_{N_c=1}(V, a_w)$ on V and a_w for droplet diameter $> 10 \mu\text{m}$ and $a_w > 0.85$ without
354 considering the dependence of homogeneous freezing temperature on $N_{total_droplets}$
355 and $\gamma_{cooling}$ in the calculations. It suggests that in most of the practical experiments
356 and for most atmospheric conditions, the time scale of $\tau_{residence}$ is shorter than
357 τ_{meta_remove} at the temperatures higher than $T_{N_c=1}(V, a_w)$ (i.e. $\tau_{residence} < \tau_{meta_remove}$,
358 when $T > T_{N_c=1}(V, a_w)$), and when the temperature of the droplets is close to
359 $T_{N_c=1}(V, a_w)$, the time scale of τ_{meta_remove} decreases strongly with temperature
360 decreases and becomes shorter than $\tau_{residence}$ of the experiments (i.e. $\tau_{residence} >$
361 τ_{meta_remove} when $T < T_{N_c=1}(V, a_w)$). This leads to the result that most of the
362 homogeneous ice nucleation process can only be observed at temperatures close to
363 $T_{N_c=1}(V, a_w)$ even though in principle, droplets can be frozen at any temperature.

364 4. Discussion

365 As mentioned in Sect. 2, the observed freezing temperatures with $\gamma_{cooling} \sim 2.5 \text{ K}$
366 min^{-1} reported in Murray et al. (2010) can be well described by $T_{N_c=1}(V, a_w)$, but it
367 also showed there is a shift of 0.5 K to 1 K in observed freezing temperatures when
368 varying the cooling rate from 2.5 K min^{-1} to 10 K min^{-1} . One possibility is that the
369 total freezing time $\tau_{freezing}$ needed to freeze a droplet at $T_{N_c=1}(V, a_w)$ is longer than

370 the time scale of $\tau_{residence}$ when $\gamma_{cooling}$ is higher than 2.5 K min^{-1} , which may be
 371 attributed to τ_{meta_remove} , $\tau_{formation}$ or $\tau_{growing}$. Without considering the experimental
 372 uncertainty associated with the thermal equilibrium time $\tau_{thermal}$, these 0.5K to 1K
 373 shifts corresponds to 3s to 6s shifts (for $\gamma_{cooling} = -10 \text{ K min}^{-1}$), which may be partly
 374 caused by $\tau_{formation} + \tau_{growing}$. Bauerecker et al. (2008) (hereafter Ba08) explored an
 375 advanced method providing time series of water droplet temperature during the entire
 376 cooling and freezing process (from supercooled water to completely freezing) using
 377 an infrared camera. The results of Ba08 showed that for the droplet sized 3mm
 378 (diameter), $\tau_{growing}$ is around 20s and $\tau_{thermal}$ is around 60s. The droplet used in
 379 Ba08 is much larger than the size normally used in the freezing experiments because
 380 of the limitation of IR camera sensitivity. If $\tau_{growing}$ linearly depends on drop radius,
 381 we may expect it to be several tenths of a second for the drops sized 10-100 μm in
 382 diameter. We suggest that the infrared camera technique should be used more widely
 383 in the future experimental studies of ice nucleation with smaller droplets, which can
 384 add significant insights into the time dependence study of ice nucleation, and clarify
 385 the importance of τ_{meta_remove} , $\tau_{formation}$ and $\tau_{growing}$ observed in the experiments. On
 386 the other hand, Koop et al. (1998) suggested that when the cooling rate is smaller than
 387 about 2 K min^{-1} , mass transport of water can take place between the frozen ice
 388 particles and supercooled droplets, but if the cooling rate is too large, it can cause an
 389 offset between the measured temperature and the actual temperature of the drops,
 390 which can both cause a bias of the observed freezing temperatures. Therefore, we
 391 suggest that in future experimental studies, in order to precisely measure $\frac{\partial T_f}{\partial \gamma_{cooling}}$,
 392 potential biases at high cooling rate and the shift caused by $\tau_{formation} + \tau_{growing}$ should

393 be better constrained. Since Koop et al. (1998) and Murray et al. (2010) showed
394 different dependencies of homogeneous freezing temperatures on $\gamma_{cooling}$, future
395 experiments should reexamine and perform the same experiments for $\gamma_{cooling} > 2.5$ K
396 min^{-1} . The results shown in Fig. 1 and Fig. 4 suggest that the time consideration may
397 be more important when droplet volume and water activity are low where the
398 experimental data show considerable inconsistency (i.e. $a_w < 0.85$ and $d < 10\mu\text{m}$),
399 and future experiments are suggested to emphasize these droplet size and water
400 activity ranges.

401 5. Summary

402 The limitation of our method proposed here is that the time dependence and the
403 stochastic feature of homogeneous freezing temperature cannot be considered because
404 the Boltzmann distribution applied here is a average distribution and does not provide
405 any information regarding time. Combining the well-known Boltzmann distribution
406 function for the mean number of critical embryos $N_{c_mean}(V, a_w, T)$ and their
407 formation energy $\Delta F_c(T, a_w)$ from CNT formulae, $T_{N_c=1}(V, a_w)$ is derived as a
408 function of volume and water activity of water droplets. With the comparison made in
409 Sect. 3.1 to 3.2, it can be summarized that under most atmospheric conditions,
410 homogeneous freezing temperatures can be well described by the new approximation
411 $T_{N_c=1}(V, a_w)$ proposed here without considering information of the applied cooling
412 rate (i.e. time dependence) and the number of droplets used in the experiment (i.e.
413 stochastic feature) for $d > 10\mu\text{m}$ and $a_w > 0.85$. Future experimental study is
414 suggested to focus on the homogeneous freezing process of droplets with high solute

415 concentration ($a_w < 0.85$) and small volume ($d < 10\mu\text{m}$). The experimental spread
416 in homogeneous freezing temperatures of water droplets may be partly explained by
417 the size distribution of droplets used in the experiments. The advantage of our
418 approximation in the cloud modeling is “the temperature history” of droplets is not
419 required to calculate the homogeneous freezing temperature as it is when using the ice
420 nucleation rate (i.e. Eq. (7-71) in Pruppacher and Klett, 1997). When using the ice
421 nucleation rate $J(T(t))$, the complete temperature history of droplets is needed to
422 calculate the integration of $J(T(t))$ with respect to time in order to consider the time
423 dependence and the stochastic feature, which can introduce considerable complexity
424 in cloud modeling. However, based on the experimental studies of homogeneous
425 freezing temperature collected and discussed in our study, we suggest in most of the
426 practical experiments and realistic atmospheric conditions (i.e. $\gamma_{cooling} < 20 \text{ K min}^{-1}$),
427 the time dependence and the stochastic feature of homogeneous freezing temperature
428 may be a secondary factor compared to the effect of volume and water activity for
429 droplet diameter $> 10 \mu\text{m}$ and $a_w > 0.85$. The approximation proposed here is
430 relatively simpler to be implemented into cloud models and may improve the
431 representation of homogeneous ice nucleation in the atmosphere.

432

433

434

435

436

437

438 **Acknowledgements**

439 **The authors gratefully appreciate helpful discussion with Marcia Baker, Daniel**
440 **Cziczo and Sarvesh Garimella who provided important insight and guidance for**
441 **this study. Two anonymous reviewers are thanked for providing important**
442 **feedback that helped to improve the paper. The authors thank Thomas Koop for**
443 **his help in supplying the data in Figure 4.**

444

445 **References**

446 Abbatt, J. P., Benz, S., Cziczo, D. J., Kanji, Z., Lohmann, U. and Mohler, O.: Solid
447 ammonium sulfate aerosols as ice nuclei: a pathway for cirrus cloud formation,
448 Science, 313, 1770-1773, 1129726 [pii], 2006.

449

450 Alpert, P. A., Aller, J. Y., and Knopf, D. A.: Initiation of the ice phase by marine
451 biogenic surfaces in supersaturated gas and supercooled aqueous phases, Phys. Chem.
452 Chem. Phys., 13, 19882–19894, 2011.

453 Baker, M. and Baker, M.: A new look at homogeneous freezing of water, Geophys.
454 Res. Lett., 31, L19102, doi:10.1029/2004GL020483, 2004.

455 Barahona, D.: Analysis of the effect of water activity on ice formation using a new
456 thermodynamic framework, Atmospheric Chemistry and Physics, 14, 7665-7680,
457 2014.

458

459 Bauerecker, S., Ulbig, P., Buch, V., Vrbka, L. and Jungwirth, P.: Monitoring ice
460 nucleation in pure and salty water via high-speed imaging and computer simulations,
461 The Journal of Physical Chemistry C, 112, 7631-7636, 2008.

462 Black, S.: Simulating nucleation of molecular solids, P. Roy. Soc. A, 463, 2799–2811,
463 2007.

464 Bourne, J. and Davey, R.: The role of solvent-solute interactions in determining
465 crystal growth mechanisms from solution: I. The surface entropy factor, J. Cryst.
466 Growth, 36, 278–286, 1976.

467 Benet, J., MacDowell, L. G. and Sanz, E.: A study of the ice–water interface using the
468 TIP4P/2005 water model, *Physical Chemistry Chemical Physics*, 16, 22159-22166,
469 2014.

470

471 Bertram, A. K., Koop, T., Molina, L. T. and Molina, M. J.: Ice formation in (NH₄)
472 2SO₄-H₂O particles, *The Journal of Physical Chemistry A*, 104, 584-588, 2000.

473

474 Bigg, E. K.: The supercooling of water, *Proc. Phys. Soc. B*, 66, 688– 694, doi:
475 10.1088/0370-1301/66/8/309, 1953.

476

477 Brewer, A. W. and Palmer, H. P.: Freezing of supercooled water, *Proc. Phys. Soc. B*,
478 64, 765–773, 1951.

479 Broto, F. and Clause, D.: A study of the freezing of supercooled water dispersed
480 within emulsions by differential scanning calorimetry, *J. Phys. C Solid State*, 9(23),
481 4251, doi: 10.1088/0022-3719/9/23/009, 1976.

482

483 Carte, A.: The freezing of water droplets, *Proc. Phys. Soc. B*, 69(10), 1028–1037,
484 1956.

485 Cziczo, D. and Abbatt, J.: Deliquescence, efflorescence, and supercooling of
486 ammonium sulfate aerosols at low temperature: Implications for cirrus cloud
487 formation and aerosol phase in the atmosphere, *Journal of Geophysical Research:*
488 *Atmospheres* (1984–2012), 104, 13781-13790, 1999.

489 Dufour, L. and Defay, R.: *Thermodynamics of clouds*, Academic Press, New York,
490 USA, 1963.

491 Duft, D. and Leisner, T.: Laboratory evidence for volume-dominated nucleation of ice
492 in supercooled water microdroplets, *Atmospheric Chemistry and Physics*, 4,
493 1997-2000, 2004.

494

495 Earle, M., Kuhn, T., Khalizov, A. and Sloan, J.: Volume nucleation rates for
496 homogeneous freezing in supercooled water microdroplets: results from a combined
497 experimental and modelling approach, *Atmospheric Chemistry and Physics*, 10,
498 7945-7961, 2010.

499 Espinosa, J., Sanz, E., Valeriani, C., and Vega, C.: Homogeneous ice nucleation
500 evaluated for several water models, *J. Chem. Phys.*, 141, 18C529, doi:
501 10.1063/1.4897524, 2014.

502 Hoffer, T. E.: A laboratory investigation of droplet freezing, *J. Meteorol.*, 18, 766-778,
503 1961.

504

505 Hu, Y., Rodier, S., Xu, K., Sun, W., Huang, J., Lin, B., Zhai, P., and Josset, D.:
506 Occurrence, liquid water content, and fraction of supercooled water clouds from
507 combined CALIOP/IIR/MODIS measurements, *J. Geophys. Res.-Atmos.*, 115(19),
508 doi: 10.1029/2009JD012384, 2010.

509 Ickes, L., Welti, A., Hoose, C., and Lohmann, U.: Classical nucleation theory of
510 homogeneous freezing of water: thermodynamic and kinetic parameters, *Phys. Chem.*
511 *Chem. Phys.*, 17, 5514-5537, 2015.

512 Jones, D. and Chadwick, G.: Experimental measurement of solid-liquid interfacial
513 energies: The ice-water-sodium chloride system, *J. Cryst. Growth*, 11, 260-264, 1971.

514

515 Kay, J., Tsemekhman, V., Larson, B., Baker, M. and Swanson, B.: Comment on
516 evidence for surface-initiated homogeneous nucleation, *Atmospheric Chemistry and*
517 *Physics*, 3, 1439-1443, 2003.

518

519 Khvorostyanov, V. I. and Curry, J. A.: Critical humidities of homogeneous and
520 heterogeneous ice nucleation: Inferences from extended classical nucleation theory,
521 *Journal of Geophysical Research: Atmospheres* (1984–2012), 114(D4), 2009.

522

523 Knopf, D. A. and Lopez, M. D.: Homogeneous ice freezing temperatures and ice
524 nucleation rates of aqueous ammonium sulfate and aqueous levoglucosan particles for
525 relevant atmospheric conditions, *Physical Chemistry Chemical Physics*, 11,
526 8056-8068, 2009.

527

528 Knopf, D. A. and Rigg, Y. J.: Homogeneous ice nucleation from aqueous
529 inorganic/organic particles representative of biomass burning: Water activity, freezing
530 temperatures, nucleation rates, *J. Phys. Chem. A*, 115, 762–773, 2011.

531 Koop, T., Luo, B., Tsias, A. and Peter, T.: Water activity as the determinant for
532 homogeneous ice nucleation in aqueous solutions, *Nature*, 406, 611-614, 2000.
533

534 Koop, T., Ng, H. P., Molina, L. T. and Molina, M. J.: A new optical technique to
535 study aerosol phase transitions: The nucleation of ice from H₂SO₄ aerosols, *The*
536 *Journal of Physical Chemistry A*, 102, 8924-8931, 1998.
537

538 Kuhns, I. and Mason, B.: The supercooling and freezing of small water droplets
539 falling in air and other gases, *Proceedings of the Royal Society of London. Series*
540 *A. Mathematical and Physical Sciences*, 302, 437-452, 1968.
541

542 Landau, L. D. and Lifshitz, E. M.: *Statistical Physics, Part I*, Pergamon, Oxford, UK,
543 1980.
544

545 Langham, E. and Mason, B.: The heterogeneous and homogeneous nucleation of
546 supercooled water, *Proceedings of the Royal Society of London. Series*
547 *A. Mathematical and Physical Sciences*, 247, 493-504, 1958.
548

549 Larson, B. H. and Swanson, B. D.: Experimental investigation of the homogeneous
550 freezing of aqueous ammonium sulfate droplets, *The Journal of Physical Chemistry A*,
551 110, 1907-1916, 2006.
552

553 McDonald, J. E.: Homogeneous nucleation of supercooled water drops, *J. Meteorol.*,
554 10, 416-433, 1953.
555

556 Mossop, S.: The freezing of supercooled water, *P. Phys. Soc. Lond. B*, 68(4), 193, doi:
557 10.1088/0370-1301/68/4/301, 1955.

558 Murphy, D. and Koop, T.: Review of the vapour pressures of ice and supercooled
559 water for atmospheric applications, *Q. J. R. Meteorol. Soc.*, 131, 1539-1565, 2005.
560

561 Murray, B., Broadley, S., Wilson, T., Bull, S., Wills, R., Christenson, H. and Murray,
562 E.: Kinetics of the homogeneous freezing of water, *Physical Chemistry Chemical*
563 *Physics*, 12, 10380-10387, 2010.
564

565 Niedermeier, D., Shaw, R., Hartmann, S., Wex, H., Clauss, T., Voigtländer, J. and
566 Stratmann, F.: Heterogeneous ice nucleation: exploring the transition from stochastic
567 to singular freezing behavior, 11, 8767-8775, 2011.
568

569 Pound, G. M., Madonna, L. and Peake, S.: Critical supercooling of pure water
570 droplets by a new microscopic technique, *J. Colloid Sci.*, 8, 187-193, 1953.
571

572 Prenni, A. J., Wise, M. E., Brooks, S. D. and Tolbert, M. A.: Ice nucleation in sulfuric
573 acid and ammonium sulfate particles, *Journal of Geophysical Research: Atmospheres*
574 (1984–2012), 106, 3037-3044, 2001.
575

576 Pruppacher, H. and Klett, J.: *Microphysics of clouds and precipitation*, 2nd Edn.,
577 Kluwer Academic Publishers, Boston, MA, 1997

578 Pruppacher, H.: A new look at homogeneous ice nucleation in supercooled water
579 drops, *J. Atmos. Sci.*, 52, 1924-1933, 1995.
580

581 Riechers, B., Wittbracht, F., Hütten, A. and Koop, T.: The homogeneous ice
582 nucleation rate of water droplets produced in a microfluidic device and the role of
583 temperature uncertainty, *Physical Chemistry Chemical Physics*, 15, 5873-5887, 2013.
584

585 Rosenfeld, D., and Woodley, W. L.: Deep Convective Clouds with Sustained
586 Supercooled Liquid Water down to -37.5C. *Nature* 405, 440–42, 2000.
587

588 Sadvovskii, M. V.: *Statistical Physics. De Gruyter Studies in Mathematical Physics.*
589 Berlin: De Gruyter, 2012.
590

591 Spaepen, F.: A structural model for the solid-liquid interface in monatomic systems,
592 *Acta Metallurgica*, 23, 729–743, 1975.

593

594 Stan, C. A., Schneider, G. F., Shevkoplyas, S. S., Hashimoto, M., Ibanescu, M., Wiley,
595 B. J. and Whitesides, G. M.: A microfluidic apparatus for the study of ice nucleation
596 in supercooled water drops, *Lab on a Chip*, 9, 2293-2305, 2009.
597

598 Vali, G.: Ice Nucleation-Theory: A Tutorial, NCAR/ASP 1999 Summer Colloquium,
599 1999.

600

601 Zobrist, B., Koop, T., Luo, B., Marcolli, C., and Peter, T.: Heterogeneous ice
602 nucleation rate coefficient of water droplets coated by a nonadecanol monolayer, J.
603 Phys. Chem. C, 111, 2149–2155, 2007.

604

605

606

607

608

609

610

611

612

613

614

615

616

617

618

619

620

621

References	Diameter (μm)	T_f (K)	Diameter Range (μm)	Range of freezing temperatures (K)	Cooling rate	Uncertainty (K)
Pound et al. (1953)	30 ⁺	233.15 ^a	[10 50]	[231.15 235.15]	n/a	n/a
Mossop (1955)	530 ⁺	238.65 ^a	[220 840]	[238.65 242.15]	0.5K/ min	0.2
Carte (1956)	15 ⁺	236.25 ^a	[10 20]	[235.15 237.15]	1K/min	0.2
	231.3 ^d	238.45 ^b	n/a	n/a	0.5K/min	0.2
	279.4 ^d	238.55 ^b	n/a	n/a	0.5K/min	0.2
	292.9 ^d	238.35 ^b	n/a	n/a	0.5K/min	0.2
	321.9 ^d	238.45 ^b	n/a	n/a	0.5K/min	0.2
	362.2 ^d	238.55 ^b	n/a	n/a	0.5K/min	0.2
	427.3 ^d	238.65 ^b	n/a	n/a	0.5K/min	0.2
	469.7 ^d	238.55 ^b	n/a	n/a	0.5K/min	0.2
	498.2 ^d	238.95 ^b	n/a	n/a	0.5K/min	0.2
	567.3 ^d	238.95 ^b	n/a	n/a	0.5K/min	0.2
	623.6 ^d	238.85 ^b	n/a	n/a	0.5K/min	0.2
	718.5 ^d	238.85 ^b	n/a	n/a	0.5K/min	0.2
	818.1 ^d	238.95 ^b	n/a	n/a	0.5K/min	0.2
	965.2 ^d	239.15 ^b	n/a	n/a	0.5K/min	0.2
	1179.8 ^d	239.45 ^b	n/a	n/a	0.5K/min	0.2
1408.4 ^d	239.65 ^b	n/a	n/a	0.5K/min	0.2	
Langham and Mason (1958)	66.1 ^d	237.35 ^a	n/a	n/a	0.33K/min	n/a
	92.3 ^d	237.65 ^a	n/a	n/a	0.33K/min	n/a
	115.3 ^d	238.15 ^a	n/a	n/a	0.33K/min	n/a
	144 ^d	238.25 ^a	n/a	n/a	0.33K/min	n/a
	171.8 ^d	238.15 ^a	n/a	n/a	0.33K/min	n/a
	270.5 ^d	238.55 ^a	n/a	n/a	0.33K/min	n/a
Hoffer (1961)	110 ⁺	236.55 ^a	[100 120]	[235.65 238.15]	1K/min	0.5
	130 ⁺	237.25 ^a	[125 145]	[235.65 238.15]	1K/min	0.5
Kuhns and Mason (1967)	1 ^d	233.05 ^a	n/a	n/a	6K/min	0.1
	5 ^d	234.65 ^a	n/a	n/a	6K/min	0.1
	8 ^d	235.15 ^a	n/a	n/a	6K/min	0.1
	10 ^d	235.45 ^a	n/a	n/a	6K/min	0.1
	20 ^d	236.15 ^a	n/a	n/a	6K/min	0.1
	30 ^d	236.75 ^a	n/a	n/a	6K/min	0.1

	40 ^d	237.05 ^a	n/a	n/a	6K/min	0.1
	50 ^d	237.25 ^a	n/a	n/a	6K/min	0.1
	60 ^d	237.35 ^a	n/a	n/a	6K/min	0.1
	70 ^d	237.45 ^a	n/a	n/a	6K/min	0.1
	80 ^d	237.55 ^a	n/a	n/a	6K/min	0.1
	90 ^d	237.65 ^a	n/a	n/a	6K/min	0.1
	100 ^d	237.65 ^a	n/a	n/a	6K/min	0.1
	120 ^d	237.65 ^a	n/a	n/a	6K/min	0.1
Broto and Clause (1976)	3 ^d	234.35 ^a	n/a	n/a	1.25K/min	0.5
Cziczo and Abbatt (1999)	0.35 ^d	234.15 ^d	n/a	n/a	n/a	n/a
Bertram et al. (2000)	8.3 ⁺	235 ^a	[5.6 11.0]	n/a	10k/min	1.5
Prenni et al. (2001)	0.6 ⁺	234.95 ^d	n/a	n/a	1K/increment	0.2
Larson and Swanson (2006)	40 ⁺	237.15 ^a	[30 50]	n/a	n/a	n/a
Stan et al. (2009)	80 ^d	236.25 ^a	n/a	[235.35 237.15]	2~100K/sec	0.21
Earle et al. (2010)	2 ⁺	236.35 ^a	[0.8 4]	[236 236.75]	n/a	n/a
	3.4 ⁺	236.35 ^a	[1.2 10]	[236 236.75]	n/a	n/a
	5.8 ⁺	236.15 ^a	[2 14]	[235.5 236.75]	n/a	n/a
Murray et al. (2010)	25 ⁺	236.25 ^a	[10 40]	[235.9 236.7]	2.5K/min	0.6
	25 ⁺	236.05 ^a	[10 40]	[234.75 237.75]	5K/min	0.6
	25 ⁺	235.75 ^a	[10 40]	[236.45 237.75]	7.5K/min	0.6
	25 ⁺	235.51 ^a	[10 40]	[234.45 237.75]	10K/min	0.6
Riechers et al. (2013)	53 ^m	236.65 ^c	[35 71]	[236.55 237.44]	1K/min	0.3
	63 ^m	236.65 ^c	[33 93]	[236.49 237.5]	1K/min	0.3
	82 ^m	236.85 ^c	[58 106]	[236.67 237.63]	1K/min	0.3
	85 ^m	237.15 ^c	[67 103]	[236.93 237.77]	1K/min	0.3
	96 ^m	237.35 ^c	[63 129]	[236.89 237.91]	1K/min	0.3

622 Table 1. Information regarding the details of the homogeneous ice nucleation
623 experiments used in the comparison, including the size, the freezing temperature, as
624 well as the cooling rate and uncertainty of the experiments. Homogeneous freezing
625 temperature T_f , <a>: freezing temperature when half of the water droplets freezing
626 $T_{50\%}$, : freezing temperature when 95% of the water droplets freezing $T_{95\%}$, <c>:
627 freezing temperature when most of the droplets freezing (peak signal) T_{Mode} , and <d>:
628 not defined or provided by the experiments. Diameter of water droplets used in the
629 experiments, <+> median size, <m> mean size, and <d> not provided by the

630 experiments.

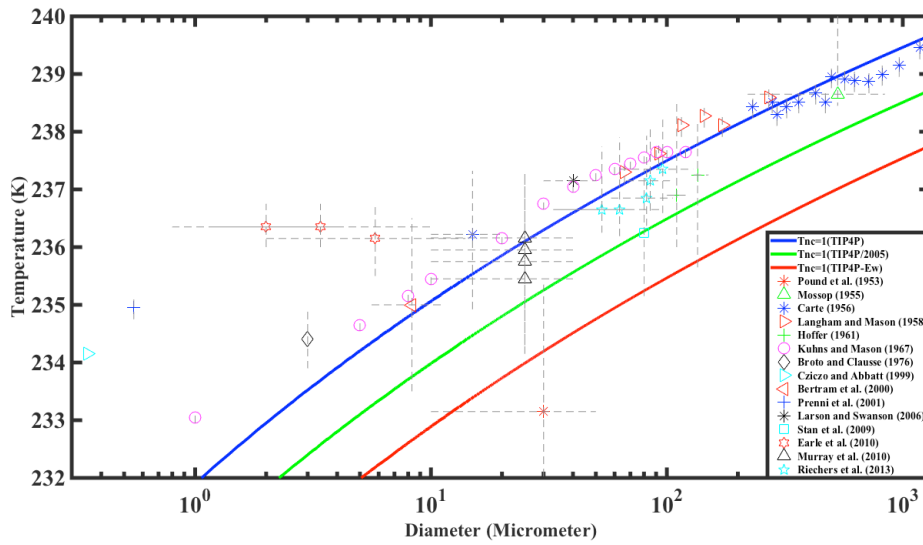
631

Diameter $\mu\pm\sigma$	96±11(μm)		85±6 (μm)		82±8 (μm)	
	Experiment values (K)	$T_{N_c=1}$ (K)	Experiment values (K)	$T_{N_c=1}$ (K)	Experiment values (K)	$T_{N_c=1}$ (K)
T_f^{onset}	237.91± 0.2	237.74	237.77± 0.2	237.53	237.63± 0.2	237.55
$T_f^{10\%}$	237.87± 0.2	237.59	237.76± 0.2	237.43	237.63± 0.2	237.42
$T_f^{50\%}$	237.4± 0.3	237.46	237.28± 0.3	237.34	237.13± 0.3	237.31
$T_f^{90\%}$	236.89± 0.3	237.31	236.93± 0.3	237.25	236.67± 0.3	237.18
T_f^{end}	N/A	237.05	N/A	237.11	N/A	236.97
Diameter $\mu\pm\sigma$	63±10 (μm)		53±6 (μm)			
	Experiment values (K)	$T_{N_c=1}$ (K)	Experiment values (K)	$T_{N_c=1}$ (K)		
T_f^{onset}	237.50± 0.2	237.43	237.44± 0.2	237.17		
$T_f^{10\%}$	237.46± 0.2	237.23	237.40± 0.2	237.02		
$T_f^{50\%}$	236.94± 0.3	237.05	236.94± 0.3	236.88		
$T_f^{90\%}$	236.49± 0.3	236.83	236.55± 0.3	236.72		
T_f^{end}	N/A	236.4	N/A	236.46		

632 Table 2. Comparison between the experimental results of the fraction experiment

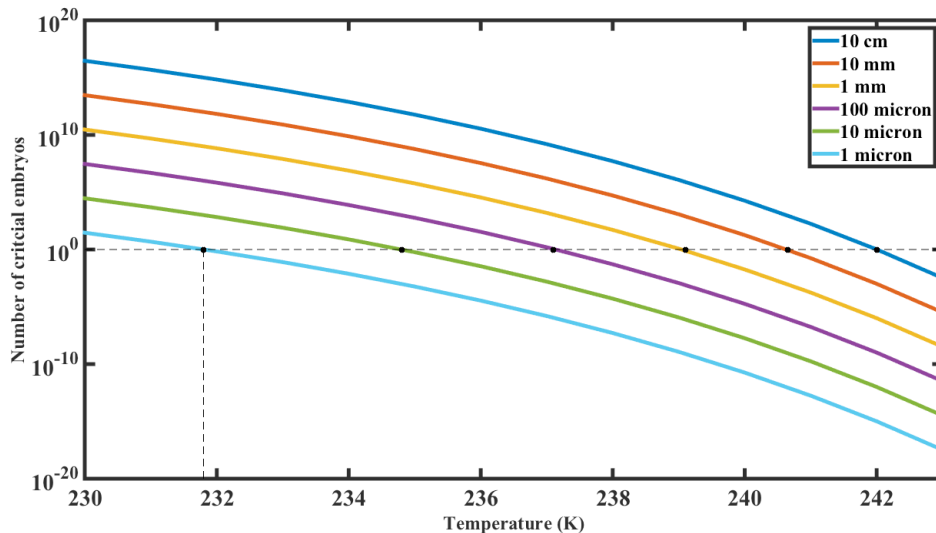
633 from Riechers et al. (2013) and the theoretical estimates $T_{N_c=1}$ derived here.

634



635

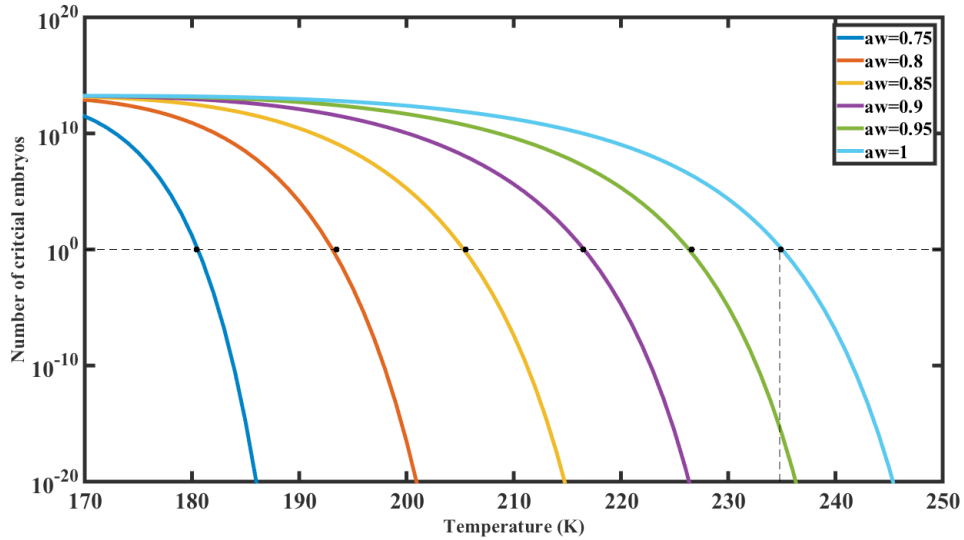
636 Figure 1. Freezing temperatures of pure water droplets: comparison between the
 637 approximations $T_{N_c=1}(V, a_w = 1)$ and the collected experimental data. Experimental
 638 data: the uncertainties and ranges of the drop size and the freezing temperatures are
 639 presented by the dotted line if information is provided by the studies (details in Table
 640 1). The approximations $T_{N_c=1}(V, a_w = 1)$: blue line - $\sigma_{i/w,e}$ from TIP4P model, green
 641 line - $\sigma_{i/w,e}$ from TIP4P/2005 model and red line - $\sigma_{i/w,e}$ from TIP4P- Ew model.



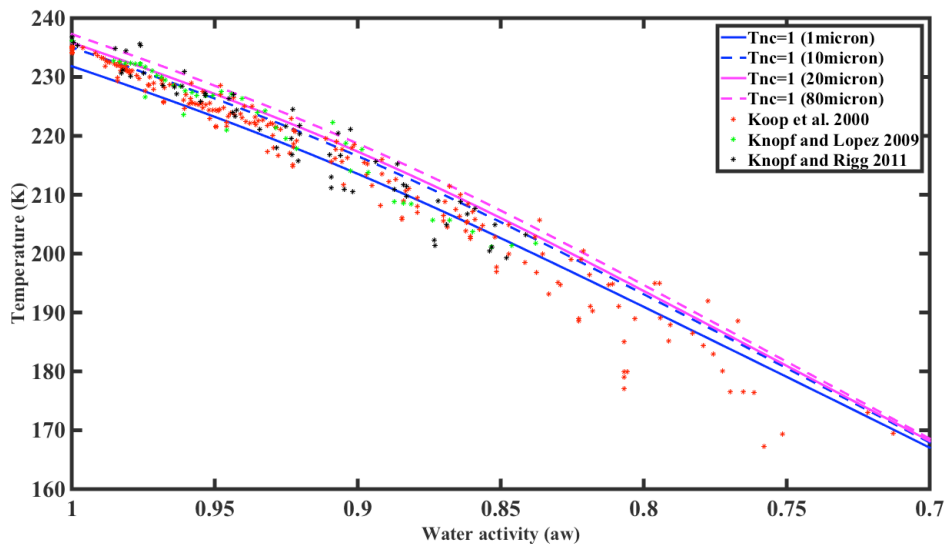
642

643 Figure 2. Mean number of critical embryos N_{c_mean} (by Eq. (1)) in a pure water
 644 droplet ($a_w = 1$) with different size (diameter) as a function of temperature. Solid

645 circle: the approximations $T_{N_c=1}(V, a_w)$ derived by Eq. (2) (using $\sigma_{i/w,e}$ from TIP4P
 646 model).

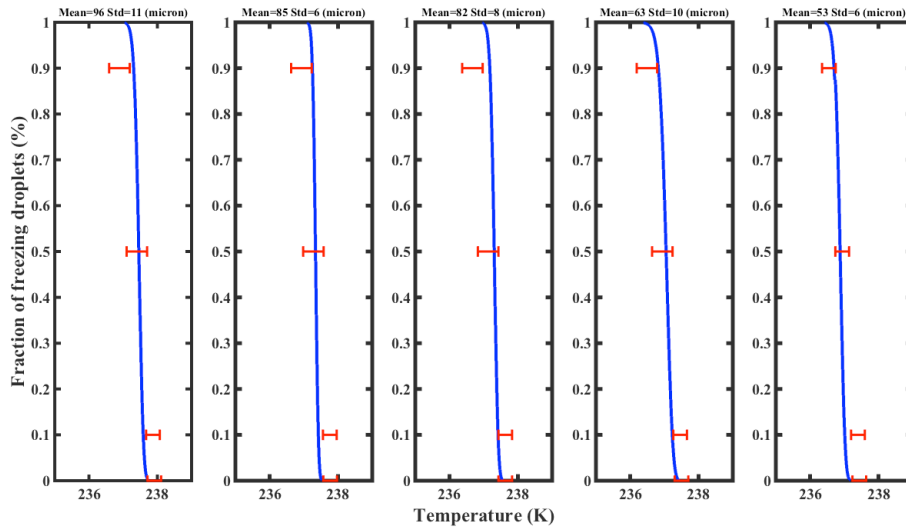


647
 648 Figure 3. Mean number of critical embryos N_{c_mean} (by Eq. (1)) in a solution droplet
 649 (diameter=1 μ m) with different water activity as a function of temperature. Solid circle:
 650 the approximations $T_{N_c=1}(V, a_w)$ derived by Eq. (2) (using $\sigma_{i/w,e}$ from TIP4P
 651 model).



652
 653 Figure 4. Comparison between the experimental data of freezing temperatures of
 654 solution droplets (Koop et al., 2000; Knopf and Lopez, 2009; Knopf and Rigg, 2011)

655 and the approximation $T_{N_c=1}(V, a_w)$.



656

657 Figure 5. Comparison between the experimental results of the fraction experiment
658 from Riechers et al. (2013) and the theoretical estimates derived here. Red:
659 experimental results with uncertainties from Riechers et al. (2013). Blue: theoretical
660 estimates ($\sigma_{i/w,e}$ from TIP4P model).